Molecular Cell, Volume *68*

Supplemental Information

The Role of N-α-acetyltransferase 10 Protein in DNA Methylation and Genomic Imprinting

Chen-Cheng Lee, Shih-Huan Peng, Li Shen, Chung-Fan Lee, Ting-Huei Du, Ming-Lun Kang, Guo-Liang Xu, Anup K. Upadhyay, Xiaodong Cheng, Yu-Ting Yan, Yi Zhang, and Li-Jung Juan

SUPPLEMENTAL INFORMATION

Supplemental Information includes seven figures and seven tables.

Supplemental Tables

Table S1 (related to Figure 1). *Naa10*-KO Mice Show Reduced Birthrate. Birthrates of mice with six different *Naa10* genotypes from *Naa10*-heterozygous (-/X) female mice crossed with WT (X/Y) male or *Naa10*-KO male (-/Y) mice were calculated. Total 48 and 41 mice from *Naa10*-heterozygous female mice crossed with WT male and *Naa10*-KO male mice were obtained, respectively. *Naa10*-KO male mice showed a birthrate of 15-17%, which is lower than the expected 25%. A lower birthrate of 12% was also observed for $Naa10^{-/-}$ female mice. The *P*-value was calculated by the chi-square test.

Table S2 (related to Figure 1). Naa10p-KO Mice Show Partial Embryonic Lethality.
Embryonic lethality was estimated in 7 litters from $Naa10^{-/X}$ female mice crossed with WT male (Litter 1 ~ 7) or *Naa10*-KO male (Litter 8 ~ 14) mice. Number with brackets indicates the amount of dead embryos. Embryos of 35% of *Naa10*-KO males (n=23 from 13 litters) and 27% of *Naa10*-KO females (n=11 from 5 litters) died with developmental defects during embryonic days 12.5-14.5. In addition, 18% embryonic lethality was observed for heterozygous $Naa10^{-/x}$ embryos (n=11 from 6 litters), but no lethality was observed for heterozygous $Naa10^{x/-}$ embryos (n=16 from 6 litters). Images of the embryos of 2 representative litters (Litter 1 and Litter 14) are shown in figure S1B.

Table S3 (related to Figure 1). Naa10p-KO Mice Develop Hydrocephalus Brain. Percentages of hydrocephalic *Naa10*-KO mice with dome-shaped skull are shown. Images of 2 representatives of the *Naa10*-KO mice with dome-shaped skull are shown in figure S1E.

Table S4 (related to Figure 2). Naa10p-KO Deregulates Imprinted Gene Expression in Mouse ESCs.

The expression of imprinted genes in the RNA-seq results from figure 2 is shown (Fold change > 1.5 & FPKM > 0.4). Red: up-regulated genes in KO cells. Green: down-regulated genes in KO cells. Fold change = FPKM of KO / average FPKM of WT#1 and WT#2.

Table S5 (related to STAR METHODS). Primers for Genotyping and Quantitative PCR.

Table S6 (related to STAR METHODS). Primers for Chromatin Immunoprecipitation.

Table S7 (related to STAR METHODS). Primers for Bisulfite Sequencing, EMSA Probes, and Site-directed Mutagenesis.

Supplemental Figures

Figure S1 (related to Figure 1). Generation and Characterization of *Naa10*-KO Mice.

(A) Generation of *Naa10*-KO mice. Top: Schematic illustration of gene targeting strategy used to generate *Naa10*-KO mouse ESCs. A 17.7 kb genomic fragment of *Naa10* was subcloned from a BAC clone (Sanger Institute, UK) into the PL235 plasmid, followed by insertion of loxp into the first and sixth introns and the neomycin resistance gene (*Neo*) cassette flanked by FRT into the sixth intron before loxp (Lee et al., 2001), by which exon 2 to 6 and *Neo* cassette were flanked by loxp sites. The resulting construct was linearized and electroporated into R1 ES cell (129 Sv/Ev) to generate *Naa10*-KO mice (see STAR METHODS). Bottom left: Southern blot confirmation of *Naa10* deletion. Analysis of WT ($Naa10^{X/X}$) and *Naa10*-heterozygous ($Naa10^{-/X}$) female mice is shown. Bottom right: Western blotting shows that Naa10p is undetectable in the *Naa10*-KO ($Naa10^{-/Y}$) MEF.

(B) Naa10p-KO mice show partial embryonic lethality. Images of the embryos at 13.5 dpc of 2 representative litters from *Naa10*-heterozygous female mice crossed with WT male (Litter 1) or *Naa10*-KO male (Litter 14) mice are shown.

(C) Positive correlation between embryo size and placenta weight in defective *Naa10*-KO female embryos. Embryo size and placenta weight were measured for embryonic day 13.5 embryos of WT ($Naa10^{X/X}$, n=6) and mutant ($Naa10^{-/X}$, n=10;

Naa10$^{-/-}$, n=7), derived from *Naa10*$^{-/X}$ females crossed with WT or *Naa10*-KO males. Representative images of embryos (#161, #166 and #167) and their placentae are shown. Embryo size is plotted vs. placenta weight for each individual. The correlation (R^2) and the p-value for the Pearson analysis are shown.

(D) *Naa10* KO results in placental defects in female embryos. Representative images of haematoxylin and eosin-stained female WT (#161) and *Naa10*-KO (#167) placentae at 13.5 dpc are shown. Regions in black rectangles are enlarged in the lower panels. De, decidual; Ch, chorionic plate; Gi, trophoblast giant cells; La; labyrinthine zone; Sp, spongioblast.

(E) *Naa10*-KO mice spontaneously develop hydrocephalus. Left: Representative images of Naa10p-KO mice with dome-shaped skull. Right: Histological analysis of brain coronal section. The *Naa10*-KO mice with short life span show enlarged lateral ventricle of hemisphere and significantly dilated third ventricle. Results are from two representative mice (4 and 5 weeks old) of WT, *Naa10*-KO without dome-shaped (ds) skull, and *Naa10*-KO with ds skull.

Figure S2 (related to Figure 2). Naa10p KO Deregulates Developmental Genes including Imprinted Genes in Mouse ESCs.

(A) Naa10p KO does not alter morphology of mouse ESCs. Phase-contrast images of three independent clones of WT (*Naa10*$^{X/Y}$) and *Naa10*-KO (*Naa10*$^{-/Y}$) ESCs cultured in N2B27 medium supplemented with Mek inhibitor PD325901, Gsk3 inhibitor Chir99021, and leukemia inhibitory factor (LIF) are shown.

(B) Naa10p KO does not alter the expression of pluripotency marker genes. mRNA levels of *Nanog* and *Oct4* in three independent WT and *Naa10*-KO ESC clones were examined by RT-qPCR. Error bars represent standard deviation determined from triplicate PCR reactions.

(C) Naa10p KO deregulates developmental genes in mouse ESCs. Heatmaps and GO term analysis of Naa10p-regulated genes are shown. Differentially expressed genes from two clones each of WT (*Naa10*$^{X/Y}$) and *Naa10*-KO (*Naa10*$^{-/Y}$) hybrid ESCs used in figure 2 were analyzed by RNA-seq. 540 and 1002 genes were up (red)- or down (green)-regulated in both KO ESCs, respectively, [fragments per kilobase of exon per million reads mapped (FPKM) > 0.4, fold change > 1.5].

(D) Naa10p KO increases gene expression from the imprinted allele in ESCs. Biological repeats (WT#2 and KO#2) for figure 2E are shown.

(E) Imprinted genes regulated by Naa10p, Zfp57 and Trim28. Van diagram comparison of the differentially expressed imprinted genes in a *Zfp57*-KO (Quenneville et al., 2011) and two *Trim28*-KO mouse ESCs (Cheng et al., 2014) with those differentially expressed in two *Naa10*-KO ESCs (**Figure 2C and Table S4**). For RNA-seq data, imprinted genes with fold change > 1.5 and FPKM > 0.4 are shown. For microarray, imprinted genes with fold change > 1.5 are shown. Number with brackets indicates numbers of total imprinted genes changed in the category. Genes with * are those affected in both *Naa10*-KO ESCs. Genes with # are those affected in both *Trim28*-KO ESCs.

Figure S3 (related to Figure 3). Naa10p KO Causes DNA Hypomethylation without Altering DNA Methyltransferase and Demethylase Levels.

(A) Naa10p KO dysregulates allele-specific imprinted gene methylation in ESCs. Biological repeats (WT#2 and KO#2) for figure 3A are shown.

(B) Naa10p KO results in global DNA hypomethylation. Shown are the mean DNA methylation levels of two wild-type (WT#1 and WT#2) and *Naa10*-knockout (KO#1 and KO#2) mESCs in various genic and repetitive sequences, and in subcategories of LTR repeats.

(C) Naa10p KO does not alter the nuclear protein levels of DNA methyltransferases, demethylases, Zfp57 and Trim28 in ESCs. Protein levels of indicated genes in the nuclear extracts of WT and *Naa10*-KO ESCs were analyzed by western blotting. *Dnmt*-TKO, mESCs depleted of Dnmt1/3a/3b.

(D) Naa10p KO does not disrupt the interaction between Dnmt1 and Uhrf1 in ESCs. Co-immunoprecipitation followed by western blot analysis shows that Uhrf1 is co-immunoprecipitated with Dnmt1 Ab in both WT and *Naa10*-KO ESCs but not mESCs depleted of Dnmt1 (*Dnmt1*-KO). IP, immunoprecipitation.

Figure S4 (related to Figure 4). Naa10p KO Barely Affects Dnmt3a/3b Activities but Impairs Dnmt1 Binding to Multiple ICRs/DMRs in Mouse ESCs.

(A) Naa10p effect on Dnmt3a/3b activities in nuclear extracts of mouse ESCs is limited. Nuclear extracts from two WT, two *Naa10*-KO or the *Dnmt*-TKO ESCs were incubated with non-methylated double-stranded DNA oligonucleotides and

[^{3}H]-S-adenosyl-L-methionine, followed by determination of radioactivity of the DNA oligonucleotides and western blotting (bottom). After subtracting the background signal of *Dnmt*-TKO cells, the relative Dnmt activity from each sample was normalized to the mean activity of WT replicates (middle). Data were presented as mean ± SD from biological repeats. Asterisks indicate statistical difference calculated by two-tail t-test, **, $p < 0.01$. The figure shows that total Dnmt activity in the nuclear extracts was reduced by only 26% when a 34 bp non-methylated DNA oligo was used as the substrate. Because Dnmt1 can also methylate non-methylated DNA *in vitro* (Yokochi and Robertson, 2001), the Naa10p KO-mediated down-regulation of Dnmt3a/3b activities, if any, should have been less than 26%.

(B) Cell cycle-sorted WT and Naa10p-KO mESCs. mESCs fixed with formaldehyde and stained with propidium iodide were analyzed for DNA content (PI) and cell size (FSC-A), followed by cell sorting. Numbers indicate the percentage/purity of each subset of cells.

(C) Naa10p KO impairs Dnmt1 binding to multiple ICRs/DMRs during S phase in mouse ESCs. Biological repeats (WT#2 and KO#2) for figure 4C are shown. Error bars represent standard deviation determined from triplicate PCR reactions.

(D) ChIP-qPCR analyses of Zfp57 occupancy at five representative ICRs/DMRs in WT#1 and KO#1 ESCs are shown. Error bars represent standard deviation determined from triplicate PCR reactions.

(E) Dnmt1 binding to non-imprinted regions is reduced in Naa10p-KO mESCs. ChIP-qPCR analyses of Dnmt1 occupancy at retrotransposon (IAP), repeat element (LINE) and four representative gene promoters in WT and Naa10p-KO mESC replicates are shown. Error bars represent standard deviation determined from triplicate PCR reactions. Asterisks indicate statistical difference calculated by two-tailed t-test, *, $p<0.05$; **, $p<0.01$.

Figure S5 (related to Figure 5). Naa10p Co-localizes with Dnmt1 at Multiple ICRs/DMRs in Mouse ESCs.

Biological repeats (WT#2 and KO#2) of figure 5A are shown. Error bars represent standard deviation determined from triplicate PCR reactions. Asterisks indicate statistical difference calculated by two-tailed t-test, *, $p<0.05$; **, $p<0.01$.

Figure S6 (related to Figure 6). Analysis of Naa10p Binding to DNA in mESCs.

(A) Naa10p preferentially binds to distal intergenic regions. Pie charts show the genomic distribution of Naa10p occupancy in mESCs (right) as well as background annotation (left, mm9). The percentage of Naa10p occupancy at each genomic region is indicated. Distal promoter, 1-3 kb upstream of transcription start site (TSS). Proximal promoter, < 1 kb upstream of TSS. Immediate downstream, < 1 kb of transcription end site (TES). Proximal downstream, 1-3 kb downstream of TES. n, number of Naa10p peaks.

(B) Naa10p binds to both parental alleles at non-imprinting regions. Genome browser views of two representative loci of non-imprinted regions show Naa10p binding peaks in WT (#1 and #2) and KO#1 ESCs. The ChIP-seq density profiles shown were normalized to density per million total reads with 25-bp resolution. Blue boxes: genes. Maternal B6 (red), paternal JF1 (blue).

(C) Naa10p-bound sites are enriched for DNA methylation. Barplot comparing the mean DNA methylation levels of Naa10p-bound and -unbound regions in WT ESCs, the results of the integrated analysis of Naa10p ChIP-seq and RRBS are shown. Shown in each bar is the average DNA methylation of all CpGs calculated.

(D) ICRs/DMRs bound by Naa10p are enriched for imprinted allele-specific SNPs. ICRs/DMRs ChIPed by Naa10p Ab from WT#1 ESC were analyzed by Sanger sequencing. Asterisks indicate SNPs on the imprinted allele.

Figure S7 (related to Figure 7). WT Naa10p, but Not the Human Disease-associated Mutants, Directly Binds to *H19*-ICR and Nucleosomes.

(A) Naa10p specifically binds to the mouse *H19*-ICR. The binding of recombinant hNaa10p to the biotin-labeled 189 bp ChIP region of mouse *H19*-ICR was analyzed by EMSA in the absence or presence of anti-hNaa10p or cold probe. hNaa10p amount: 2 μg (lanes 2-5 and 7-9). The Naa10p binding was specific because it could be disrupted with the Naa10p Ab and competed away with cold DNA probe. Lanes with the controls of antibody and BSA alone were eliminated from the original image to save space.

(B) Mutations outside the GCXGXG motif do not disrupt Naa10p binding. The binding of recombinant hNaa10p to the biotin-labeled 20-mer oligo of mouse

H19-ICR with or without mutations indicated in red was analyzed by EMSA. hNaa10p amount: 1 μg (lanes 2 and 6); 2 μg (lanes 3 and 7); 4 μg (lanes 4 and 8). Lanes using DNA probe with irrelevant mutations were eliminated from the original image to save space.

(C) WT Naa10p, but not clinical-relevant mutants, binds to nucleosomes. EMSA of WT and mutant hNaa10p binding to the biotin-labeled 216 bp Widom DNA reconstituted with HeLa nucleosomes is shown. hNaa10p amount: 0.5 μg (lanes 3, 6, 9 and 12); 1 μg (lanes 4, 7, 10 and 13); 2 μg (lanes 5, 8, 11 and 14).

(D) The GCXGXG motif is enriched at ICRs/DMRs. The GCXGXG motif in both ICRs/DMRs and the 10 kb-flanked regions was extracted. Frequency of motif per kb is shown for 10 representative ICRs/DMRs. Circle, maternally imprinted genes. Triangle, paternally imprinted genes. The -10k-flanked region of *H19* is known to harbor a somatic DMR.

Table S1 (related to Figure 1)

Reduced birthrate of *Naa10*-KO mice

	Naa10 genotype of progeny					
	X/Y	-/Y	X/X	-/X	X/-	-/-
Expected probability	25%	25%	25%	25%	-	-
-/X x X/Y	35%	15%	29%	21%		
P=0.025	(17/48)	(7/48)	(14/48)	(10/48)		
Expected probability	25%	25%	-	-	25%	25%
-/X x -/Y	32%	17%			39%	12%
P=0.0002	(13/41)	(7/41)			(16/41)	(5/41)

Table S2 (related to Figure 1)

Lethality of *Naa10*-KO embryo at 12.5 ~ 14.5 dpc

	Naa10 of breeder	*Naa10* genotype of embryo					
		X/Y	-/Y	X/X	-/X	X/-	-/-
Litter 1		1	1(1)	2	2		-
Litter 2		1	1(1)	4	1		-
Litter 3		3	2	1	0		-
Litter 4	-/X x X/Y	3	0	0	1(1)		-
Litter 5		2	2	3	1		-
Litter 6		1	3(1)	2	3(1)		-
Litter 7		1	2(1)	2	3		-
Litter 8		2	2(1)	-		3	0
Litter 9		1	3(1)	-		0	3
Litter 10		1	1	-		2	2(1)
Litter 11	-/X x -/Y	2	1	-		1	0
Litter 12		3	1	-		3	3(1)
Litter 13		1	3(1)	-		4	1
Litter 14		2	1(1)	-		3	2(1)
Lethality		0% (0/24)	35% (8/23)	0% (0/14)	18% (2/11)	0% (0/16)	27% (3/11)

Table S3 (related to Figure 1)

***Naa10*-KO live birth mice with dome-shaped skull**

Genotype of *Naa10*				
X/Y	-/Y	X/X	-/X & X/-	-/-
0% (0/61)	34% (11/32)	0% (0/24)	4% (2/55)	31% (4/13)

Table S4 (related to Figure 2C)

		Fold Change			
Imprinted Genes	**Expressed Parental Allele**	**WT#1**	**WT#2**	**KO#1**	**KO#2**
Htr2a	M	0.838	1.162	9.553	0.666
Dlk1	P	1.075	0.925	8.583	2.318
Axl	M	0.936	1.064	5.411	0.799
Peg10	P	1.073	0.927	4.100	2.847
Wt1	M	0.930	1.070	3.922	1.266
Peg13	P	1.087	0.913	3.654	1.802
Osbpl5	M	0.974	1.026	3.627	0.854
Rtl1	P	0.997	1.003	3.484	3.954
Tfpi2	M	0.763	1.237	3.002	0.062
Tnfrsf23	M	0.973	1.027	2.211	0.837
Pon3	M	1.096	0.904	2.140	1.149
Ndn	P	1.008	0.992	2.117	1.414
H13	M	0.971	1.029	2.076	0.833
Kcnq1ot1	P	1.241	0.759	1.976	1.897
Pon2	M	1.016	0.984	1.888	1.195
Mest	P	1.014	0.986	1.868	1.653
Sfmbt2	P	0.945	1.055	1.810	2.585
Nnat	P	1.027	0.973	1.805	1.447
Impact	P	0.964	1.036	1.718	1.158
Klf14	M	1.116	0.884	1.664	1.031
Meg3	M	0.97	1.029	1.646	0.978
Blcap	M	0.997	1.003	1.615	1.056
H19	M	1.131	0.869	1.612	2.202
Casd1	M	0.962	1.038	1.598	1.736
Dcn	M	0.917	1.083	1.597	0.258
Peg3	P	1.036	0.964	1.588	1.587
Gnas	M	0.993	1.007	1.561	0.937
Gatm	M	0.985	1.015	1.551	1.004
Snrpn	P	1.005	0.994	1.533	1.557
Sgce	P	0.997	1.003	1.500	1.561
Phlda2	M	0.983	1.017	1.463	1.121
Magel2	P	1.051	0.949	1.410	0.800
Mcts2	P	0.967	1.033	1.327	1.007

Zdbf2	P	0.983	1.017	1.259	0.908
Ube3a	M	1.069	0.931	1.235	1.207
Begain	P	1.142	0.858	1.197	1.002
Calcr	M	0.877	1.123	1.195	0.554
Cmah	M	1.010	0.990	1.138	0.979
Atp10a	M	0.969	1.031	1.126	1.222
Mkrn3	P	1.146	0.854	1.078	0.741
Zfp64	P	1.035	0.965	1.058	1.338
Nap1l4	M	0.977	1.023	1.029	0.876
Plagl1	P	1.010	0.990	1.027	1.091
Jade1	P	0.991	1.009	1.021	0.914
Slc38a4	P	0.993	1.007	0.992	1.027
Pde4d	P	1.040	0.960	0.977	1.282
Tbc1d12	P	1.028	0.972	0.976	0.716
Ipw	P	0.944	1.056	0.972	0.922
Xlr3b	M	0.880	1.120	0.951	0.732
Copg2	M	0.967	1.033	0.906	0.897
Peg12	P	0.824	1.176	0.873	1.138
Igf2r	M	1.008	0.992	0.838	0.657
Grb10	M	0.984	1.016	0.829	0.355
Zrsr1	P	1.016	0.984	0.794	0.888
Trappc9	M	0.970	1.030	0.777	0.891
Ampd3	M	1.067	0.933	0.769	1.015
Cdkn1c	M	1.180	0.820	0.751	0.755
Commd1	M	0.984	1.016	0.705	0.830
Phactr2	M	1.015	0.985	0.698	1.051
Dio3	P	1.058	0.942	0.673	0.554
Igf2	P	1.384	0.616	0.639	0.598
Qpct	M	1.087	0.913	0.630	0.837
Ascl2	M	0.538	1.462	0.546	0.801
Ppp1r9a	M	1.012	0.988	0.527	0.564
Cobl	M	0.997	1.003	0.520	0.912
Dhcr7	M	1.041	0.959	0.507	1.000
Slc22a18	M	1.036	0.964	0.479	0.894
Zim3	M	1.117	0.883	0.383	0.683
Mst1r	M	1.054	0.946	0.342	0.540
Art5	M	0.973	1.027	0.316	0.653

Table S5 (related to STAR METHODS)

Primers for Genotyping			
Name	**Direction**	**Sequence (5' to 3')**	**Position**
Naa10-CU	Forward	CTTACGGGGTGACCGTGTGA	chrX 65174147-65174128
Naa10-FD	Reverse	GCTGCAATGACTAAGAGG	chrX 65173836-65173853
Naa10-JD	Reverse	GACAACCTGGTTACTGACCA	chrX 65170767-65170786
M-Probe A	Forward	TGAGGGAGGTTAGACACTG	chrX 65163005-65163023
M-Probe A	Reverse	GTTGAGGCCAAAGAGGCTT	chrX 65163470-65163488
M-Probe B	Forward	CTGAGATCAGCAGCGGAC	chrX 65163536-65163553
M-Probe B	Reverse	CTTCCAGAGTCATAGCCCAT	chrX 65164148-65164167
Primers for Quantitative PCR			
Name	**Direction**	**Sequence (5' to 3')**	**Ref.**
Nanog	Forward	TCTTCCTGGTCCCCACAGTTT	
Nanog	Reverse	GCAAGAATAGTTCTCGGGATGAA	
Oct4	Forward	CACCATCTGTCGCTTCGAGG	
Oct4	Reverse	AGGGTCTCCGATTTGCATATCT	
H19	Forward	CCTTGTCGTAGAAGCCGTCTG	
H19	Reverse	GGGTAGCACCATTTCTTTCATCT	
Allele-specific *H19*	Forward	TCCTTTTGTTCCTTCCTTGC	Sharif et al. 2007
Allele-specific *H19*	Reverse	TGATGGACCCAGGACCTCT	Sharif et al. 2007
Kcnq1ot1	Forward	ATGGCCAGTGCCACTAGTTC	

Kcnq1ot1	Reverse	TTTGCTTTCTCGTCGTCTCA	
Allele-specific *Kcnq1ot1*	Forward	CCTCCTGCGAGTTTCTTGTC	Sharif et al. 2007
Allele-specific *Kcnq1ot1*	Reverse	TGGAACCTCCTTGGAAGATG	Sharif et al. 2007
Igf2	Forward	GTGCTGCATCGCTGCTTAC	
Igf2	Reverse	ACGTCCCTCTCGGACTTGG	
Cdkn1c	Forward	CGAGGAGCAGGACGAGAATC	
Cdkn1c	Reverse	GAAGAAGTCGTTCGCATTGGC	
Gapdh	Forward	TTGCAGTGGCAAAGTGGAG	
Gapdh	Reverse	CATGGTGGTGAAGACACCAG	

Table S6 (related to STAR METHODS)

Primers for Chromatin Immunoprecipitation			
Name	**Direction**	**Sequence (5' to 3')**	**Position or Ref.**
Peg10-DMR	Forward	TACTGACCGAATTGTGATGAG	chr6 4747860-4747880
Peg10-DMR	Reverse	CGCATGAAGCGCCTATTAGG	chr6 4748026-4748007
Peg13-DMR	Forward	AAAGGAGGCACAGAAAAAGC	ch15 72809661-72809642
Peg13-DMR	Reverse	TACAACCACAATGCGCCTAT	ch15 72809468-72809487
Kcnq1ot1-DMR	Forward	TCGAGTCCCAAGGTGAGTGG	chr7 143295500-143295481
Kcnq1ot1-DMR	Reverse	GACCCGATTCGGTTTCAGC	chr7 143295401-143295419
Mest-DMR	Forward	CGGGTGCTTGGCGAAAGCCGTCC	chr6 30736490 - 30736512
Mest-DMR	Reverse	CAAGAATTTGAGGGCGCACAGGG	chr6 30736600 - 30736622
H19-ICR	Forward	GTACAACACACATTTCTTGGG	ch7 142336826-142336807
H19-ICR	Reverse	ACTCAAAGCTTTGTCACAGC	ch7 142336636 - 142336655
Peg3-DMR	Forward	ATGGGGTCTTGGATTGGTTA	chr7 6730500 - 6730481
Peg3-DMR	Reverse	TAGTGCACCCACACTGAACC	chr7 6730308-6730327
Snrpn-DMR	Forward	TGCATACTCAAGGCCAGGTTC	chr7 60005915 - 60005935
Snrpn-DMR	Reverse	GCATATTGAAGTTACTACCAC	chr7 60006059 - 60006079
Meg3-IG-DMR	Forward	GCCTGTAACCAATAGACCCAGAG	chr12 109533876 - 109533898
Meg3-IG-DMR	Reverse	GAACACCCGATTAACTGAGCAG	chr12 109534007-109534028

IAP-LTR1	Forward	TGGTAAACAAATAATCTGCGCATGA	Di Giacomo et al., 2014
IAP-LTR1	Reverse	CACTCCCTGATTGGCTGCAG	Di Giacomo et al., 2014
IAP-LTR2	Forward	GTGAGAACGCGTCGAATAACAAT	Di Giacomo et al., 2014
IAP-LTR2	Reverse	GTGATCCGTAGTTCTGGTTCTGA	Di Giacomo et al., 2014
5'-LINE-L1	Forward	TGCGGTACATAGGGAAGCAGG	Di Giacomo et al., 2014
5'-LINE-L1	Reverse	CAAGACTCTGCTGGCAAGGTA	Di Giacomo et al., 2014
3'UTR-LINE-L1	Forward	CCAAGGAGCTAAAGGGATCTG	Di Giacomo et al., 2014
3'UTR-LINE-L1	Reverse	CCGACTAGGCCATCTTTTGAT	Di Giacomo et al., 2014
Cyp26a1	Forward	GGAGCCTCTGGTCTCCTTAG	Chr19 37697062 - 37697081
Cyp26a1	Reverse	TCCTGCTTTCGAGTTCAAAG	Chr19 37697163 - 37697182
Ereg	Forward	GGGAGTAGCCACACTAGAAG	Chr5 91074409 - 91074428
Ereg	Reverse	GTTTCCTAATGCCACCCCCC	Chr5 91074519 - 91074538
Pcdh7	Forward	GGACTCTGGCAGTCCCAGCC	Chr5 57720628 - 57720647
Pcdh7	Reverse	CTCTGGAAAGTAAACCTCAACC	Chr5 57720721 - 57720742
Rps6ka4	Forward	CCCCTGACACCCCACCCATC	Chr19 6837485 - 6837504
Rps6ka4	Reverse	GCGCCCAACCTCTTCTTAGG	Chr19 6837373 - 6837392
Primers for ChIP Followed by Sanger Sequencing			
Name	**Direction**	**Sequence (5' to 3')**	**Position**
Peg13-DMR	Forward	TGTGTGATAGCTCATCCAAGC	chr15 72809842-72809822

Peg13-DMR	Reverse	CTACAACCACAATGCGCCTA	chr15 72809467-72809486
Kcnq1ot1-DMR	Forward	CAGCGCGGGTTTCTTCTCTG	chr7 143295827-143295808
Kcnq1ot1-DMR	Reverse	GACCCGATTCGGTTTCAGC	chr7 143295401-143295419
H19-ICR	Forward	GGGTCACAAATGCCACTAGG	chr7 142581935-142581916
H19-ICR	Reverse	AGCCCATGACTATGGGATCA	chr7 142581701-142581720
Snrpn-DMR	Forward	GGACTCCTGGAAGTCAGAGC	chr7 60004742 - 60004723
Snrpn-DMR	Reverse	CCCAGACCACACAAGCTG	chr7 60004300 - 60004317
Mest-DMR	Forward	TCTGGGGTTCAGGATTAGAGA	chr6 30737845 - 30737865
Mest-DMR	Reverse	AGCAGAGGCAGCAAGCAG	chr6 30738177 - 30738160

Table S7 (related to STAR METHODS)

Primers for Bisulfite Sequencing			
Name	**Direction**	**Sequence (5' to 3')**	**Ref.**
H19-ICR	Forward	AGGGTATTTATATTTAGGATTTAAAGGAATATG	Sharif et al. 2007
H19-ICR	Reverse	TTTATCAAAAACTAACATAAACCCCTAACC	Sharif et al. 2007
Kcnq1ot1-DMR	Forward	ATTTTTGTGGTTTAGGTTTATAGAAGTAGGG	
Kcnq1ot1-DMR	Reverse	TACTCCACTCACTACCTTAATACTAACC	
Peg13-DMR	Forward	GGTTTTGTGTGATAGTTTATTTAAG	
Peg13-DMR	Reverse	TAACTCATCATTATACTACAACCAC	
Primers for the EMSA Probe and Site-directed Mutagenesis			
Name	**Direction**	**Sequence (5' to 3')**	**Ref.**
H19-ICR (189 bp)-Bio	Forward	Biotin-GTACAACACACATTTCTTGGG	
H19-ICR (189 bp)	Reverse	ACTCAAAGCTTTGTCACAGC	
hNaa10p S37P	Forward	CTTCTACCATGGCCTTCCCTGGCCCCAGCTC	Rope et al. 2011
hNaa10p V107F	Forward	CTTCAATGCCAAATATTTCTCCCTGCATGTCAGG	Popp et al. 2015
hNaa10p R116W	Forward	CATGTCAGGAAGAGTAACTGGGCCGCCCTGCAC	Popp et al. 2015

Figure S1 (related to Figure 1)

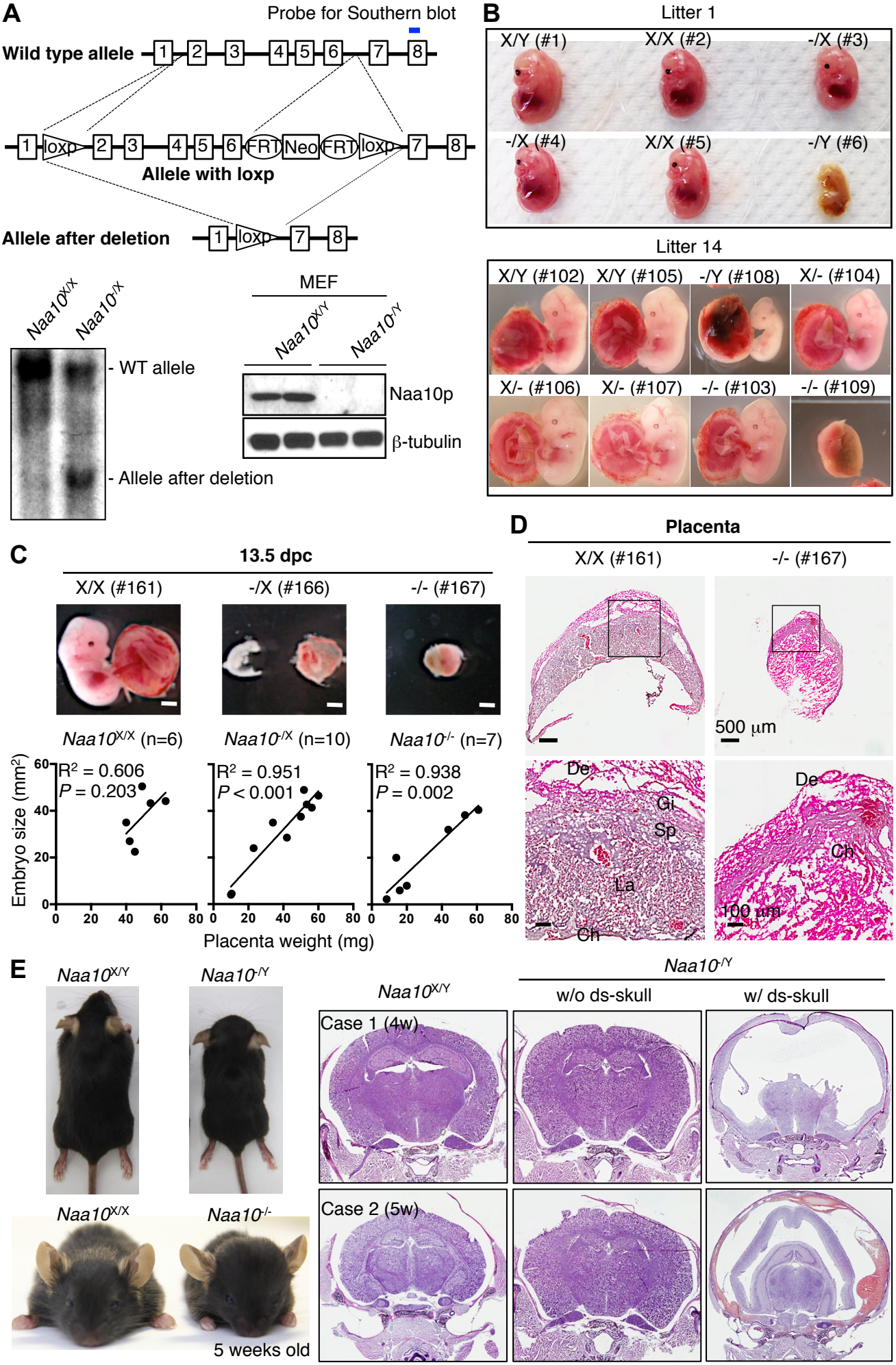

Figure S2 (related to Figure 2)

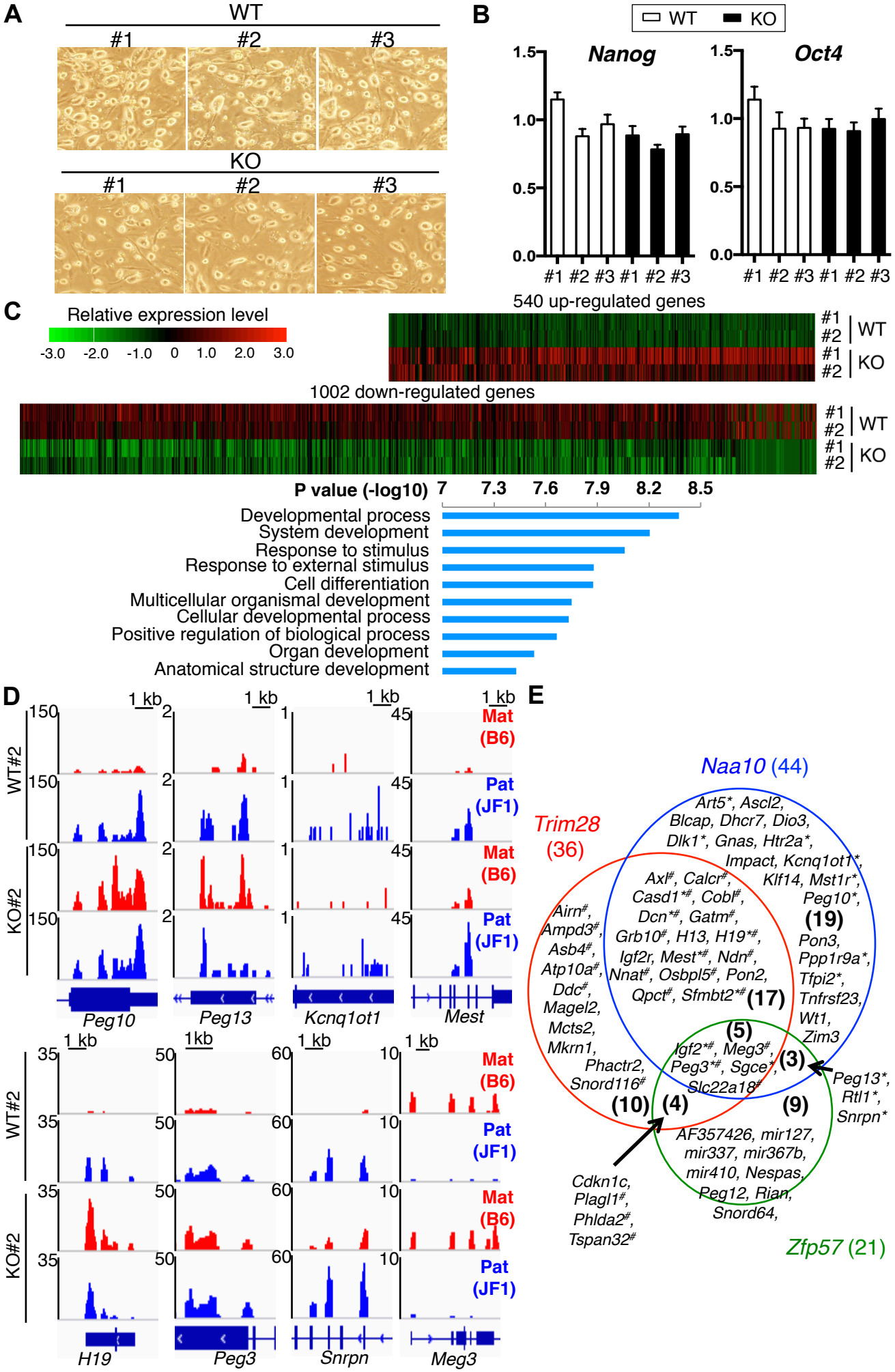

Figure S3 (related to Figure 3)

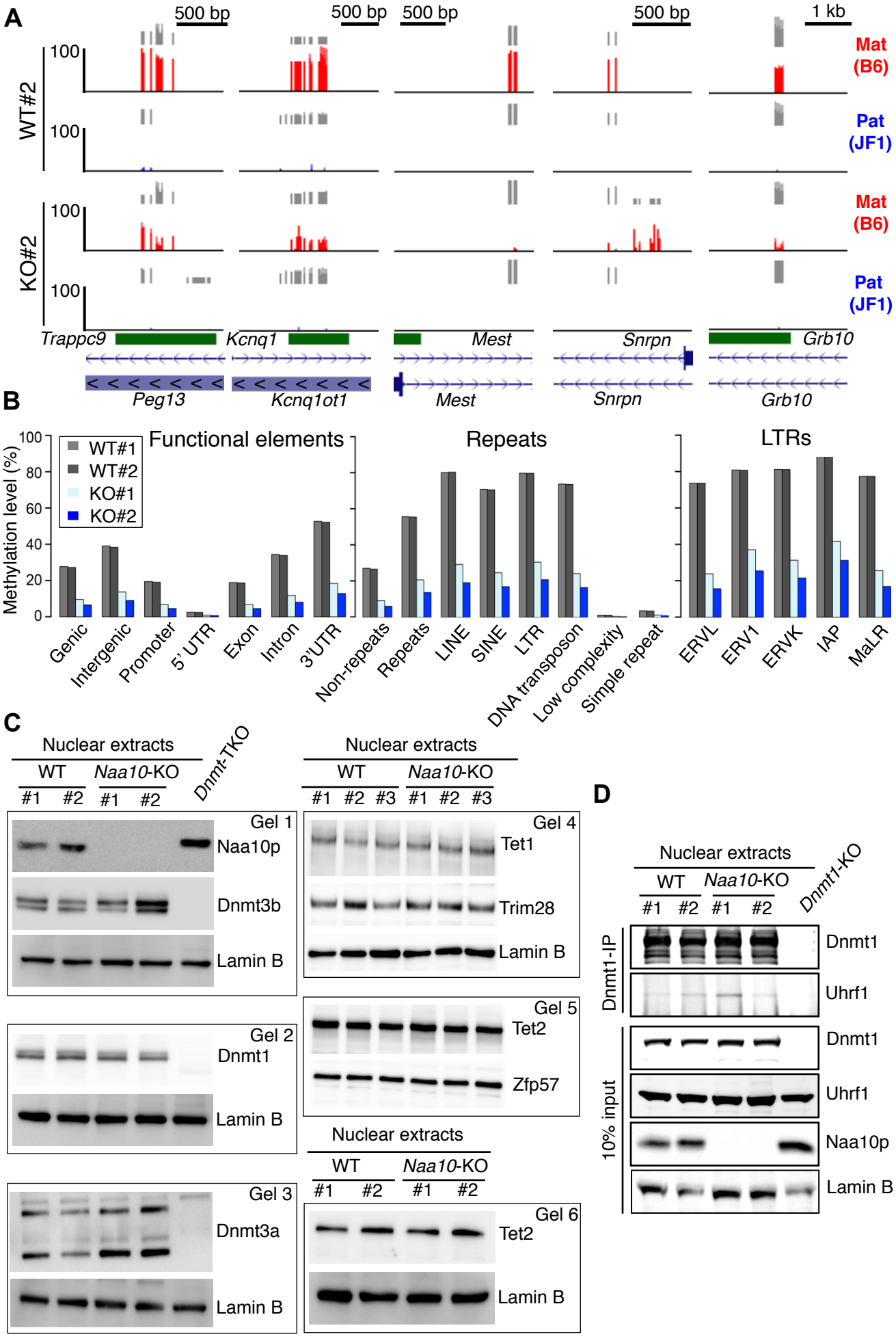

Figure S4 (related to Figure 4)

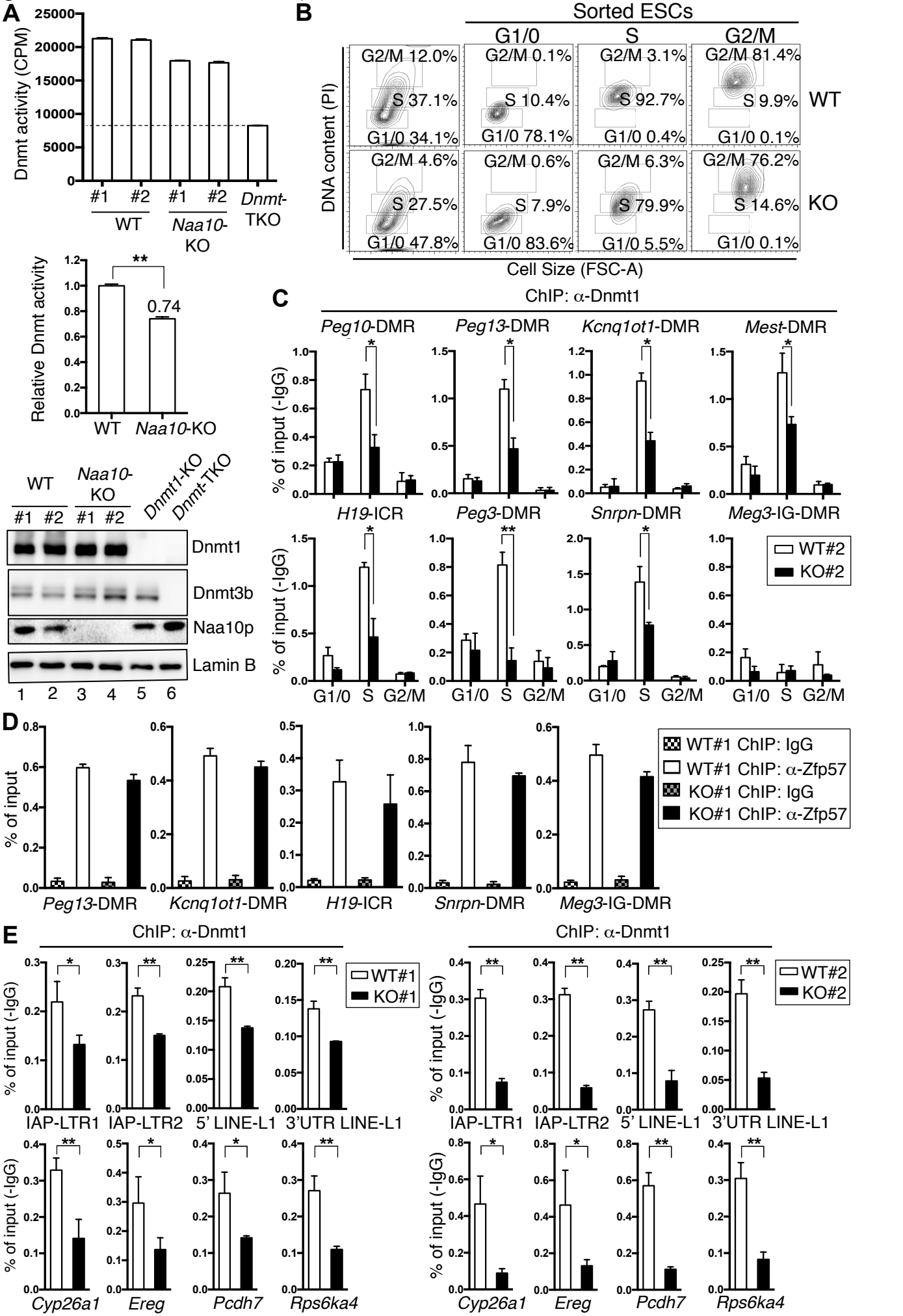

Figure S5 (related to Figures 5)

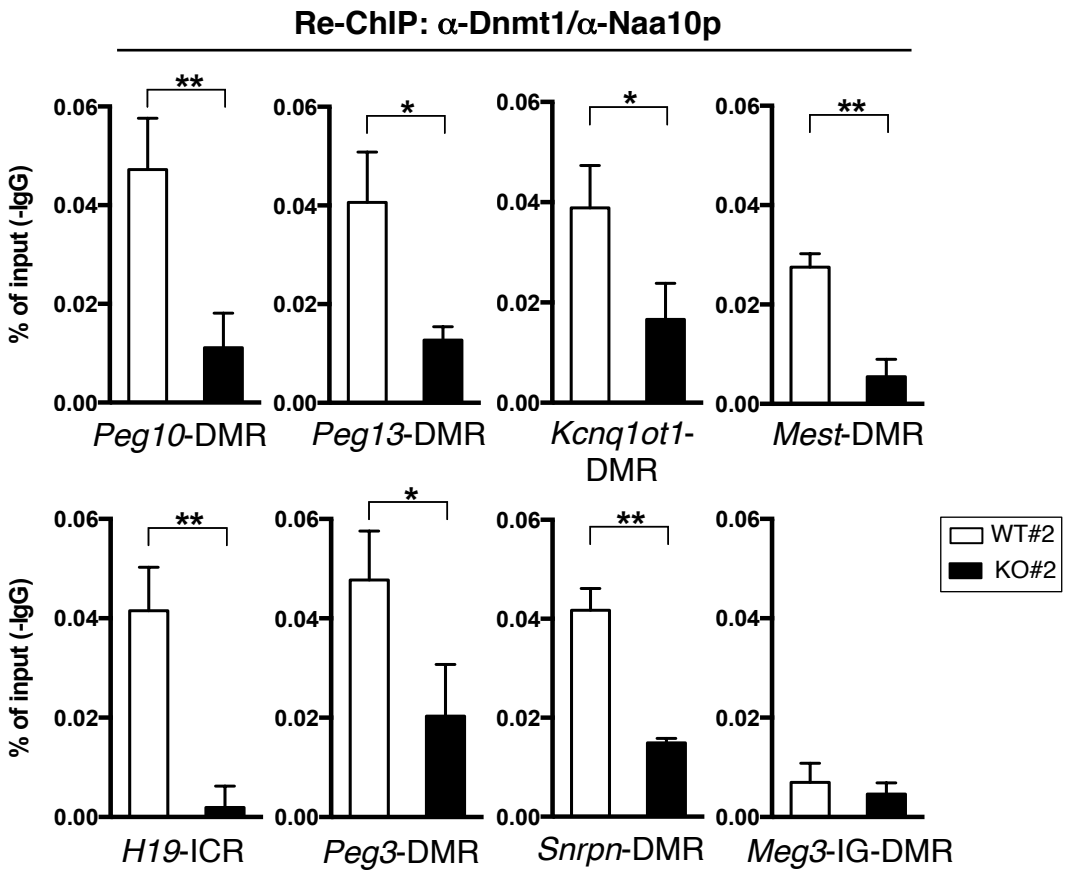

Figure S6 (related to Figure 6)

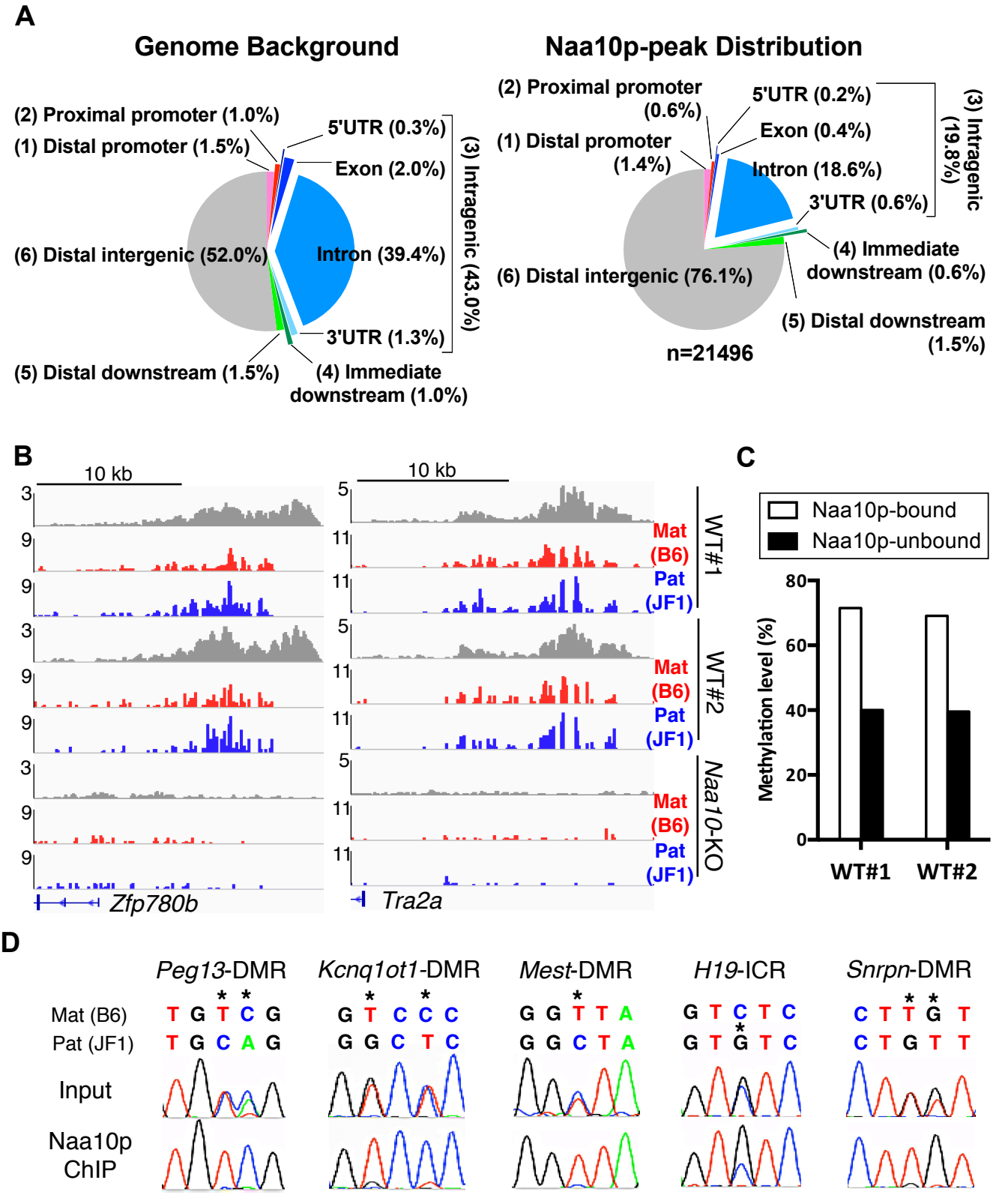

Figure S7 (related to Figure 7)